Nonequilibrium phases for driven particle systems with effective orientational degrees of freedom

C. Reichhardt and C. J. Olson Reichhardt
Theoretical Division, Los Alamos National Laboratory, Los Alamos, New Mexico 87545, USA
(Received 26 March 2009; published 26 June 2009)

We show that a rich variety of nonequilibrium phases can be realized for interacting particles moving over a periodic substrate when the particles have effective internal orientational degrees of freedom. We specifically study driven colloidal molecular crystals where it has been established that *n*-merization produces effective orientational degrees of freedom. This system exhibits a polarization effect within the pinned phase, a remarkable variety of sliding phases, and has no single particle pinning regime. Similar dynamics should occur for other driven systems with effective orientational degrees of freedom such as sliding diatomic or higher-order states.

DOI: 10.1103/PhysRevE.79.061403 PACS number(s): 82.70.Dd

I. INTRODUCTION

Extensive experimental and theoretical studies of nonequilibrium states have been performed for interacting particle systems driven over periodic and random substrates. These include theories of sliding friction [1–3], experimental [4–7] and theoretical [8–12] studies of vortex matter in superconductors, simulations of vortices in Bose-Einstein condensates [13], experiments on sliding charge-density waves [14,15], simulations [16] and experiments [17] on driven Wigner crystals, and experimental [18–23] and theoretical [24–26] studies of driven colloid particles. These systems exhibit a wide range of dynamical phases and a number of transitions including pinned to sliding states, plastic sliding to elastic sliding states, and transitions between different types of ordered and quasiordered states. Previous dynamical studies have been limited to systems in which the pointlike particles have no internal or orientational degrees of freedom. There has been some theoretical work on individual dimers moving on periodic substrates [27–30]; however, collections of interacting particles with effective orientational degrees of freedom have not been considered so far.

In this work we study the nonequilibrium driven phases for a class of systems where particle-particle interactions are known to produce effective orientational degrees of freedom. We specifically consider colloidal molecular crystals, which can be realized for colloidal particles interacting with periodic substrates when the number of colloids is equal to an integer multiple of the number of potential minima. Within each minima or trap, the colloids undergo *n*-merization which causes them to act like rigid objects such as dimers, trimers, and higher-order *n*-mers, each of which has an effective orientational degree of freedom. Since the colloids are not strictly bound into a single object but are only held together by the substrate, they do not have a true orientational degree of freedom. Orientational ordering arises due to the quadrupolar or higher-order electrostatic interactions between the *n*-mers. Depending on the number of colloids per trap, substrate symmetry, and substrate strength, the *n*-mers have been shown to exhibit ferromagnetic, antiferromagnetic, columnar, and other types of ordering [24,31–33].

We demonstrate that the effective orientational degree of freedom of the *n*-mers which favors certain orientations can compete with an external drive which tends to align the *n*-mers, producing a rich variety of nonequilibrium phenomena even for the simplest case of dimers. Within the pinned phase, the application of a biasing driving force results in a polarization effect where the dimers can align with the drive. The scaling of the velocity-force curve near the depinning transition changes significantly depending on whether the system is fully polarized or not. In the moving state, the particles can still retain their effective *n*-merization even though they are no longer confined to a single trap. We also find an intermediate disordered moving state that separates a moving aligned dimer state from a moving nonaligned state. This intermediate state appears due to a competition between the polarization effect which persists into the sliding state and the herringbone ordering preferred by the dimers. Our results should be general to a wide class of systems of particles with effective orientational or effective internal degrees of freedom driven over ordered or quasiordered substrates. It is now possible to fabricate colloidal dumbbells that can exhibit different types of orientational orderings [34] as well as more complex shapes [35]. Other systems where the driven phases described here could be observed include dimer or trimer bubbles created in systems with competing interactions found in soft matter [36] and hard condensed matter systems [37]. It should possible to impose an additional periodic substrate and a drive in these cases. Similar states should be realizable for atoms, cold molecules, or ions on tilted optical traps. In this case, the molecules have an effective orientational degree of freedom, while the ions could form *n*-mers that are similar to the colloidal molecular crystal states.

II. SIMULATION

We consider a two-dimensional system with periodic boundary conditions in the x and y directions containing N_c colloidal particles. The dynamics of a single colloid i at position $\mathbf{R}_i$ is governed by the overdamped equation of motion [9,11]

$$\eta \frac{d\mathbf{R}_i}{dt} = \mathbf{F}_i^{cc} + \mathbf{F}_i^{s} + \mathbf{F}_d, \tag{1}$$

where we set $\eta=1$. The colloid-colloid interaction force is $\mathbf{F}_i^{cc} = -\sum_{j\neq i}^{N_c} \nabla V(R_{ij})$ where the potential has a Yukawa form,

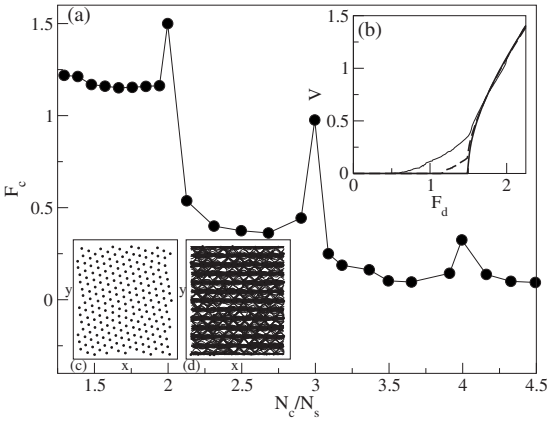

FIG. 1. (a) The critical depinning force F_c versus filling fraction N_c/N_s for a substrate with strength $A=2.5$. Peaks appear at the commensurate fillings of $N_c/N_s=2$, 3, and 4. (b) V, the average colloidal velocity per particle, vs the external drive F_d for $N_c/N_s=1.94$ (dashed line), 2 (thick line), and 2.13 (thin line). A clear depinning threshold exists which is largest at $N_c/N_s=2$. (c) The colloidal positions (black dots) and trajectories (black lines) for $N_c/N_s=2.0$ in the pinned triangular crystal (PC) state at $F_d=0.0$ and $A=0.5$. (d) Colloid positions and trajectories for $N_c/N_s=2.0$ in the moving random (MR) state at $A=1.5$ and $F_d/F_c=1.1$.

$V(R_{ij})=(E_0/R_{ij})\exp(-\kappa R_{ij})$ and where $R_{ij}=|\mathbf{R}_i-\mathbf{R}_j|$, $E_0=Z^{*2}/(4\pi\epsilon\epsilon_o a_o)$, ϵ is the solvent dielectric constant, Z^* is the effective charge, and $1/\kappa$ is the screening length. Lengths are measured in units of a_0, assumed to be on the order of a micron, forces are measured in units of $F_0=E_0/a_0$ and time is measured in units of $\tau=\eta/E_0$. The substrate force $\mathbf{F}_s$ arises from a triangular substrate with

$$\mathbf{F}_s=\sum_{i=1}^{3} A\sin\left(\frac{2\pi b_i}{a_0}\right)[\cos(\theta_i)\hat{\mathbf{x}}-\sin(\theta_i)\hat{\mathbf{y}}], \qquad (2)$$

where $b_i=x\cos(\theta_i)-y\sin(\theta_i)+a_0/2$, $\theta_1=\pi/6$, $\theta_2=\pi/2$, and $\theta_3=5\pi/6$. Here A is the relative substrate strength and there are N_s substrate minima. The initial colloidal positions are obtained through simulated annealing. The applied driving force $\mathbf{F}_d=F_d\hat{\mathbf{x}}$ represents the force that would be produced by an external electric field [23]. For each drive, we measure the average colloid velocity $V=\langle N_c^{-1}\Sigma_i^{N_c}d\mathbf{R}_i/dt\cdot\hat{\mathbf{x}}\rangle$. The depinning force F_c is defined as the value of F_d at which $V=0.025$.

III. RESULTS

In Fig. 1(a) we plot the depinning threshold F_c versus the filling factor N_c/N_s over the range $1.5<N_c/N_s<4.5$ for a system with a substrate of strength $A=2.5$. At the integer matching fields $N_c/N_s=2$, 3, and 4, there are clear peaks in the depinning threshold. This is similar to the behavior observed for vortices in superconductors with periodic pinning, where peaks in the critical current (which is proportional to the depinning force) appear when the vortex density is an integer multiple of the pinning site density [4,6,9,11]. In Fig. 1(b) we illustrate the velocity-force curves for $N_c/N_s=1.94$, 2.0, and 2.13. A clear single depinning threshold appears at

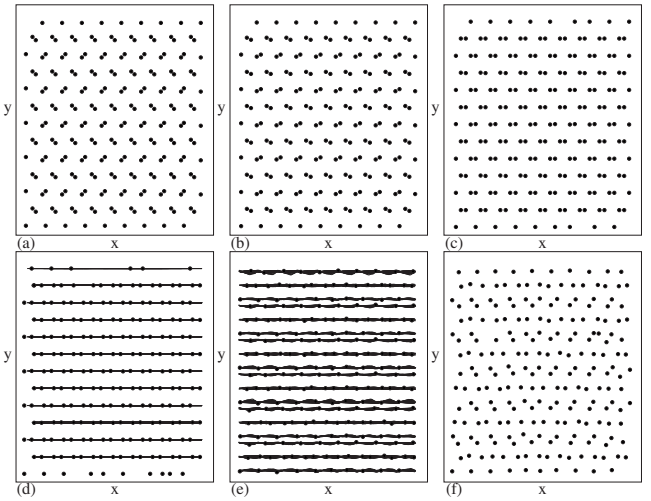

FIG. 2. The colloid positions (black dots) and trajectories (black lines) for $N_c/N_s=2.0$ and (a–d) $A=3.25$; (e and f) $A=1.5$. (a) The pinned herringbone (PHB) state at $F_d=0$. (b) The PHB at finite $F_d/F_c=0.45$ showing the onset of dimer polarization in the direction of the drive. (c) The fully polarized dimers at $F_d/F_c=0.9$ form the pinned ferromagnetic (PF) state. (d) The moving ferromagnetic (MF) state at $F_d/F_c=1.1$ where the motion is strictly one-dimensional. (e) The partially ordered moving ferromagnetic (PMF) state for $A=1.5$ at $F_d/F_c=1.5$. (f) Vortex positions only in the PMF state from panel (e) showing that every other row of dimers is aligned.

$N_c/N_s=2$, while two-step depinning transitions occur at the noninteger fillings. For $N_c/N_s=1.94$, the initial depinning occurs due to the motion of monomer defects in the dimer lattice followed by the depinning of the remaining dimers, while for $N_c/N_s=2.13$, the trimer defects in the dimer lattice depin first and then the remaining dimers depin at a higher drive.

We measure F_c versus substrate strength A for the case $N_c/N_s=2.0$ and find that there are three distinct pinned states and four moving states. In Fig. 2 we plot the colloidal configurations at different values of F_d for $A=3.25$. At $F_d=0$, the ground state is the pinned herringbone (PHB) structure shown in Fig. 2(a). For increasing F_d, the dimers become increasingly *polarized* in the direction of drive, as illustrated in Fig. 2(b) for $F_d/F_c=0.45$. At sufficiently large F_d, the dimers are completely aligned into the pinned ferromagnetic (PF) state shown in Fig. 2(c) for $F_d/F_c=0.9$. This polarization effect results when the effective orientational degree of freedom of the dimers couples to the external drive and is absent for simple point particles. After the system is fully polarized, the dimers depin directly into the moving ferromagnetic (MF) state, where the dimers align with the drive in one-dimensional channels as seen in Fig. 2(d). This shows that the polarization effect can persist in the moving phase.

The same sequence of states also appears for higher values of A. The PF-MF transition is continuous, as shown in Fig. 3(a) where we plot V versus F_d for $A=3.25$. The inset of Fig. 3(a) indicates that the velocity follows a power-law scaling, $V=(F_d-F_c)^\alpha$ with $\alpha=1/2$, with a turnover at higher F_d to a linear form. This exponent is consistent with elastic depinning in which the colloids keep the same neighbors

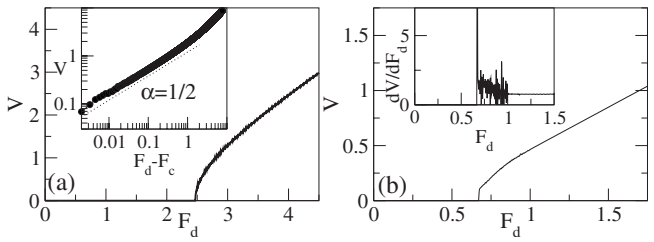

FIG. 3. (a) V vs F_d for $N_c/N_s=2.0$ and $A=3.25$ showing the continuous PF-MF depinning transition. Inset: V vs F_d-F_c in the same system indicating a power-law scaling with $\alpha=0.5$. (b) V vs F_d for $N_c/N_s=2.0$ and $A=1.5$. The depinning occurs from a PHB state to a MR state and at higher drives the colloids organize into a PMF state. Inset: dV/dF_d vs F_d for the same system. The sharp jump indicates that the depinning transition is discontinuous. The fluctuating region corresponds to the MR state and the onset of a regime with small fluctuations at $F_d>1$ corresponds to the formation of the PMF state.

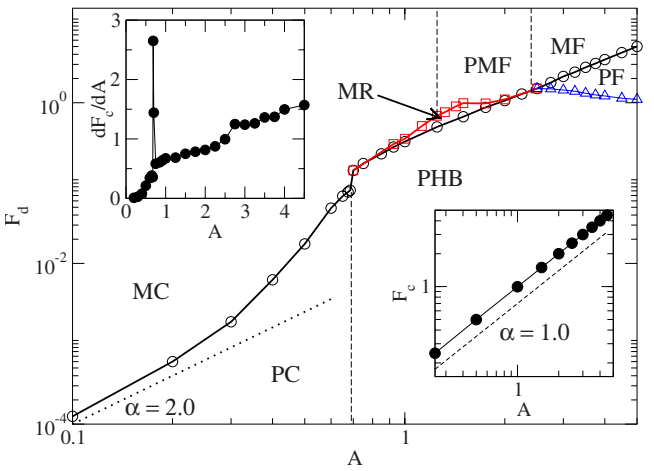

FIG. 4. (Color online) The dynamic phase diagram for F_d vs A with $N_c/N_s=2.0$. Open circles: depinning threshold. Dotted line: a fit to a power law with $\alpha=2.0$. PC, pinned triangular crystal; PHB, pinned herringbone; PF, pinned ferromagnetic; MC, moving triangular crystal; MR, moving random; MF, moving ferromagnetic; and PMF, partially ordered moving ferromagnetic. Upper left inset: dF_c/dA vs A for the depinning curve in the main panel. The sharp peak separates the PC and PHB states. Lower right inset: F_c vs A for a single isolated particle showing a linear scaling.

while moving. We observe the same velocity scaling for $A\geq 2.5$.

For $0.7<A<2.5$, the pinned system does not fully polarize and the partially polarized PHB state depins *discontinuously* into a *plastically* flowing state where the colloids can exchange neighbors and undergo a transverse diffusive behavior, as shown in Fig. 1(d). We call this the moving random (MR) state. It arises due to a competition between the polarizing effect of the driving force and the orientational ordering induced by the effective quadrupolar interaction between the dimers. In Fig. 3(b) we plot the velocity-force curve at $A=1.5$ which has a discontinuous depinning transition, as indicated by the plot of dV/dF_d versus F_d in the inset of Fig. 3(b). There is a clear sharp jump in V at the PHB-MR depinning transition, followed by a regime of fluctuating dV/dF_d which corresponds to the MR state. For $F_d>1.0$, the fluctuations are diminished when the system forms a partially ordered moving ferromagnetic (PMF) state, illustrated in Fig. 2(e) and 2(f). Here the moving colloids form a stripelike structure in which every other row of dimers is aligned with the drive. Unlike the MR state shown in Fig. 1(d), in the PMF state there is no transverse diffusion. For $A<0.7$ and $F_d=0$, the weak substrate causes the elastic energy cost of the PHB state to be too high and instead the colloids form a pinned triangular crystal (PC) state illustrated in Fig. 1(c). The PC state is only weakly pinned and the depinning occurs as a continuous elastic transition to a moving triangular crystal (MC) state.

In Fig. 4 we summarize the different states in a dynamic phase diagram for $N_c/N_s=2.0$. We plot dF_c/dA versus A in the upper inset of Fig. 4 to show how changes in F_c correlate with different phases of the system. The PHB-PC transition is marked by a discontinuous jump down in F_c when the PC phase forms, as indicated by the sharp peak in dF_c/dA. A smaller feature in dF_c/dA occurs at $A=2.5$ when the depinning changes from the discontinuous PHB-PMF transition to the continuous PF-MF transition. The PF phase forms for $A>2.5$ and the PHB-PF transition shifts to lower F_d with increasing A. Since the PHB state forms due to the effective quadrupole interaction between the dimers [32], as A increases the colloids forming each dimer are pulled closer together, reducing the quadrupole moment and facilitating the formation of the PF and MF states. The MR state appears in a narrow window between the two elastic depinning transitions PHB-MC and PHB-PMF when the competing symmetries induce a disordered phase. In the MR regime, there is a competition between the quadrupole moment which prevents the dimers from aligning into the PF state and the tendency of the external drive to align the dimers. The intermediate random phase is a feature that does not occur for systems without effective orientational degrees of freedom since in these systems, the random or plastic flow phases grow in extent as the substrate strength is increased; this is in contrast to what we observe here, where an increase in substrate strength causes the onset of an ordered phase.

For $0.7<A\leq 1.25$, the MR state orders into a MC state for increasing F_d rather than forming the PMF state. For small A, F_c exhibits a scaling $F_c\propto A^2$. A similar scaling occurs for $A>0.7$ as well. In contrast, for a single colloid moving over the periodic substrate, we find the linear behavior $F_c\propto A$ as shown in the lower inset of Fig. 4. The collective depinning behavior that occurs in the PHB state for large A likely arises because the objects that are depinning are dimers rather than single particles.

For $N_c/N_s=3.0$, we find a similar set of pinned and moving phases as shown in the dynamic phase diagram for F_d vs A in Fig. 5(a). At this filling, there is only a single pinned phase, the pinned trimer crystal (PTC) illustrated in Figs. 5(b) and 5(c) for $A=0.5$ and $A=2.5$, and so there is no discontinuous transition in F_c vs A such as that seen at the PHB-PC transition for $N_c/N_s=2.0$. In Fig. 5(a), the PTC-MC depinning transition for $A<1.0$ is elastic, while for $A>1.0$ the PTC-MR depinning transition is followed at higher drives by the organization of the colloids into either the mov-

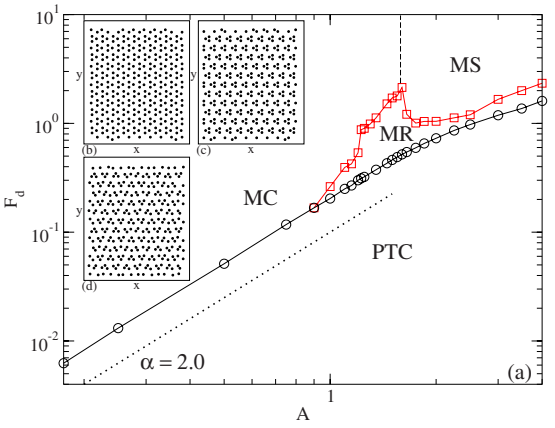

FIG. 5. (Color online) (a) The dynamic phase diagram for F_d vs A with $N_c/N_s=3.0$. Open circles: depinning threshold. PTC: pinned trimer crystal; MC: moving triangular crystal; MR: moving random; MS: moving stripe. (b) Colloid positions in PTC at $A=0.5$ and $F_d=0$. (c) Colloid positions in PTC at $A=2.5$ and $F_d=0$. The size of each trimer is reduced compared to panel (b). (d) The MS state at $A=2.5$ and $F_d=1.5$.

ing crystal (MC) state or into the moving stripe (MS) state illustrated in Fig. 5(d). In the MS state, the colloids are strictly confined to move along one-dimensional rows with no transverse diffusion. The oriented trimer structure found in the PC is lost in the MS state; however, some orientational ordering of the trimers persists in the MS state producing a zigzag structure. The MR state reaches its maximum extent at the transition between the MC and MS phases at $A=1.6$. The scaling of F_c with A is consistent with collective depinning for low A, while for $A>3.0$, there is a rollover to a more linear regime, indicative of single particle depinning. In the high-A regime, the depinning occurs via the hopping of individual colloids from well to well followed at higher drives by more general motion of all the colloids.

We expect that a similar type of phase diagram will occur for the higher-order colloidal molecular crystals. Additional phases are likely to occur at incommensurate fillings. Thermal fluctuations could produce interesting effects since it has been shown that the disordering transition depends on the substrate strength [24,31,32].

IV. SUMMARY

We have shown that a different class of driven particle systems moving over ordered substrates can be realized when the particles have an effective orientational degree of freedom. We specifically studied the case of colloidal molecular crystals which have previously been shown to exhibit effective collective orientational degrees of freedom due the formation of colloidal n-mer states. These effective orientational degrees of freedom allow phenomena such as a polarization effect in the pinned and moving states which is induced by the external drive. The polarization effect competes with the preferred orientational ordering of the n-mers, producing a remarkably rich variety of sliding phases even for the simplest case of colloidal dimers. For example, we find a dynamically induced disordered phase between the moving polarized state and the moving orientationally ordered state. The particles act like composite objects rather than like single particles, so that even at commensurate fillings, we do not find linear velocity-force curves which would be associated with single particle depinning. Our results should be general to other systems where the particles have an effective orientational degree of freedom. Examples include sliding molecule states on surfaces, ions, or molecules in tilted optical traps, and differnet types of colloidal dumbbell states.

ACKNOWLEDGMENT

This work was carried out under the auspices of the NNSA of the U.S. DOE at LANL under Contract No. DE-AC52-06NA25396.

[1] B. N. J. Persson, *Sliding Friction: Theory and Applications* (Springer, Berlin, 1998).
[2] J. Tekic, O. M. Braun, and B. Hu, Phys. Rev. E **71**, 026104 (2005).
[3] M. C. Righi and M. Ferrario, Phys. Rev. Lett. **99**, 176101 (2007).
[4] M. Baert, V. V. Metlushko, R. Jonckheere, V. V. Moshchalkov, and Y. Bruynseraede, Phys. Rev. Lett. **74**, 3269 (1995).
[5] K. Harada, O. Kamimura, H. Kasai, T. Matsuda, A. Tonomura, and V. V. Moshchalkov, Science **274**, 1167 (1996).
[6] J. I. Martín, M. Vélez, J. Nogués, and I. K. Schuller, Phys. Rev. Lett. **79**, 1929 (1997).
[7] F. Pardo, F. de la Cruz, P. L. Gammel, E. Bucher, and D. J. Bishop, Nature (London) **396**, 348 (1998).
[8] A. E. Koshelev and V. M. Vinokur, Phys. Rev. Lett. **73**, 3580 (1994).
[9] C. Reichhardt, C. J. Olson, and F. Nori, Phys. Rev. Lett. **78**, 2648 (1997).
[10] C. J. Olson, C. Reichhardt, and F. Nori, Phys. Rev. Lett. **80**, 2197 (1998).
[11] C. Reichhardt, G. T. Zimányi, and N. Grønbech-Jensen, Phys. Rev. B **64**, 014501 (2001).
[12] E. Olive and J. C. Soret, Phys. Rev. B **77**, 144514 (2008).
[13] K. Kasamatsu and M. Tsubota, Phys. Rev. Lett. **97**, 240404 (2006).
[14] R. Danneau, A. Ayari, D. Rideau, H. Requardt, J. E. Lorenzo, L. Ortega, P. Monceau, R. Currat, and G. Grubel, Phys. Rev. Lett. **89**, 106404 (2002).
[15] D. Le Bolloc'h, V. L. R. Jacques, N. Kirova, J. Dumas, S. Ravy, J. Marcus, and F. Livet, Phys. Rev. Lett. **100**, 096403 (2008).
[16] C. Reichhardt, C. J. Olson, N. Grønbech-Jensen, and F. Nori, Phys. Rev. Lett. **86**, 4354 (2001).
[17] G. A. Csathy, D. C. Tsui, L. N. Pfeiffer, and K. W. West, Phys. Rev. Lett. **98**, 066805 (2007).
[18] P. T. Korda, M. B. Taylor, and D. G. Grier, Phys. Rev. Lett.

89, 128301 (2002).
[19] D. G. Grier, Nature (London) **424**, 810 (2003).
[20] K. Mangold, P. Leiderer, and C. Bechinger, Phys. Rev. Lett. **90**, 158302 (2003).
[21] M. P. MacDonald, G. C. Spalding, and K. Dholakia, Nature (London) **426**, 421 (2003).
[22] J. Mikhael, J. Roth, L. Helden, and C. Bechinger, Nature (London) **454**, 501 (2008).
[23] A. Pertsinidis and X. S. Ling, Phys. Rev. Lett. **100**, 028303 (2008).
[24] C. Reichhardt and C. J. Olson, Phys. Rev. Lett. **88**, 248301 (2002); C. Reichhardt and C. J. Olson Reichhardt, Phys. Rev. E **71**, 062403 (2005).
[25] A. M. Lacasta, J. M. Sancho, A. H. Romero, and K. Lindenberg, Phys. Rev. Lett. **94**, 160601 (2005).
[26] A. Soba, P. Tierno, T. M. Fischer, and F. Sagués, Phys. Rev. E **77**, 060401(R) (2008).
[27] A. H. Romero, A. M. Lacasta, and J. M. Sancho, Phys. Rev. E **69**, 051105 (2004).
[28] S. Goncalves, C. Fusco, A. R. Bishop, and V. M. Kenkre, Phys. Rev. B **72**, 195418 (2005).
[29] M. Tiwari, S. Goncalves, and V. M. Kenkre, Eur. Phys. J. B **62**, 459 (2008).
[30] S. von Gehlen, M. Evstigneev, and P. Reimann, Phys. Rev. E **79**, 031114 (2009).
[31] M. Brunner and C. Bechinger, Phys. Rev. Lett. **88**, 248302 (2002).
[32] R. Agra, F. van Wijland, and E. Trizac, Phys. Rev. Lett. **93**, 018304 (2004); S. El Shawish, J. Dobnikar, and E. Trizac, Soft Matter **4**, 1491 (2008).
[33] A. Sarlah, T. Franosch, and E. Frey, Phys. Rev. Lett. **95**, 088302 (2005); A. Sarlah, E. Frey, and T. Franosch, Phys. Rev. E **75**, 021402 (2007).
[34] S. J. Gerbode, S. H. Lee, C. M. Liddell, and I. Cohen, Phys. Rev. Lett. **101**, 058302 (2008).
[35] S. C. Glotzer and M. J. Soloman, Nat. Mater. **6**, 557 (2007).
[36] B. A. Grzybowski, J. A. Wiles, and G. M. Whitesides, Phys. Rev. Lett. **90**, 083903 (2003); Y. H. Liu, L. Y. Chew, and M. Y. Yu, Phys. Rev. E **78**, 066405 (2008).
[37] M. M. Fogler, A. A. Koulakov, and B. I. Shklovskii, Phys. Rev. B **54**, 1853 (1996); E. Fradkin and S. A. Kivelson, *ibid.* **59**, 8065 (1999).